HHS Public Access

Author manuscript

IEEE Int Conf Rehabil Robot. Author manuscript; available in PMC 2015 March 09.

Published in final edited form as:

IEEE Int Conf Rehabil Robot. 2013 June ; 2013: 6650508. doi:10.1109/ICORR.2013.6650508.

A Body-Machine Interface for the Control of a 2D Cursor

Ismael Seáñez and
BME, Northwestern University Chicago, USA i-seanez@u.northwestern.edu

Ferdinando A. Mussa-Ivaldi
BME, Northwestern University PM&R, Northwestern University Chicago, USA
sandro@northwestern.edu

Abstract

This paper develops a body-machine interface for the control of a powered wheelchair using upper-body motion. Our goal was to infer a cursor's kinematics from the signals recorded from 4 Inertial Measurement Units placed on a subject's shoulders. We specified a Kalman filter measurement model that assumes the Euler angles, angular velocities, and linear accelerations of the shoulders are a stochastic linear function of the position, velocity, and acceleration of the virtual cursor. This model learned a system that encodes cursor movement along with training data. Experimental results show that taking advantage of the redundancy of the signal improves performance during a center-out reaching task. The resulting algorithm provides a platform for people with high-tetraplegia to communicate their intended motor actions with the environment using specialized assistive devices.

Keywords

Body-machine interface; inertial measurement units; Kalman filter; powered wheelchair control

I. INTRODUCTION

Injury to the cervical spinal cord causes devastating and long-lasting loss of mobility, impaired sensory function, and compromised movement coordination. Spinal cord injured individuals control assistive devices with their residual motor and sensory capacities in order to regain mobility and communicate with the environment. Current specialized interfaces like the sip-and-puff system and the head array are designed to match the residual abilities of the disabled users. However, once in place they have a fixed functionality and this places the burden of learning entirely on the user. The available interactions are strictly constrained and fail to promote learning through upper-body coordination, which is critical for people with high tetraplegia to avoid collateral effects of paralysis such as muscular atrophy, chronic pain, and to recover some of the lost mobility [1–3].

We have developed a novel approach for a system that we call the “body-machine interface”, which aims at enabling people with high-level paralysis to communicate intended

motor actions using their individual motor capacities. Simultaneous recordings of shoulder motions were acquired from four Inertial Measurement Units (IMU) attached with Velcro to the subject's shoulders. In an experimental setup analogous to [4], unimpaired subjects viewed a computer monitor and were instructed to follow a smoothly moving cursor on the screen as if controlling it with their shoulder motions. Upper-body kinematics (Euler angles, angular velocities, and linear accelerations) from shoulder motions were simultaneously recorded and logged with the position, velocity, and acceleration of the moving cursor. These data were then used to train a Kalman filter that decoded body motion (observation) into the control of a virtual cursor (state) [5]. Our approach builds on previous work with brain-machine interfaces [6], [7]. In that case spike trains recorded from cortical neurons guided the motion of a cursor on a computer monitor. Here, we consider the application of the same concept to infer a desired smooth cursor motion from upper-body kinematics. The rationale is to use a non-invasive approach to exploit the residual mobility that remains available to the paralyzed users of assistive devices.

Current brain-machine interfaces do poorly at helping subjects efficiently communicate with the environment because they are difficult to control [8–13]. Using an algorithm that exploits the abundance and redundancy of individuals' residual body motion might address this problem. Such an algorithm would use as much information as possible to "learn" the mapping and estimate the *state* from the *observation* at each point in time. However, more information is not always better, i.e. adding more noisy data might actually degrade performance of the reconstruction of cursor motion.

Here, we analyze the role of redundancy on the control of the interface. We designed an experiment to test the effectiveness of adding more information in the observation vector of the decoding algorithm. We asked subjects in three different groups to perform a reaching task by controlling with shoulder movements a cursor on a computer monitor. For each group, the "learning" and "decoding" of the algorithm was performed using different information in the observation vector. Subjects in the first group (E) used only Euler angles from the four IMUs in order to control the cursor. Subjects in the second group (EV) used angles and angular velocities, and subjects in the third group (EVA) used Euler angles, angular velocities, and linear accelerations. We compared performance between the three groups during five epochs of a center-out reaching task.

Subjects in all groups were able to learn and perform the task throughout the whole experiment, but performance varied depending on the information included in the observation vector. Subjects in the EVA group generally performed better than subjects in the other groups across all epochs. However, a learning trend was only apparent for subjects in groups E and EV. These results might suggest that subjects who are using all available body kinematics information may reach a ceiling in performance from the very first epochs.

This experiment provides us with the platform to transform residual motion into the control of a cursor. With appropriate training, the cursor characteristics can be transformed into the characteristics of a joystick that controls a wheelchair. The combination of customized interfacing and human motor learning might allow people with paralysis to improve their independence by enhancing their movement capabilities that survived the injury.

II. METHODS

A. Experimental Setup

Subjects wore an adjustable size motion vest with Velcro patches on the shoulder areas. Two MTi (Xsens) motion sensors were attached to the Velcro area for each of the subject's shoulders. The motion sensors were able to capture shoulder elevation, depression, adduction, and abduction through the combination of 3-D of freedom accelerometers and gyroscopes. Data from the sensors were sampled in real-time (Simulink, Mathworks, MA) at a rate of 50Hz.

The 24-dimensional vector ([2-Euler (Roll, Pitch) + 2-Gyroscope + 2-Accelerometer]*4 Sensors) of sensor values was mapped to the position of the cursor presented on a computer monitor via the Kalman filter approach [5] as applied by Wu et al [7].

B. Kalman Filter Algorithm

The main objective was to estimate the state of the cursor on the screen $x_k = [x, y, v_x, v_y, a_x, a_y]^T_k$ representing x-position, y-position, x-velocity, y-velocity, x-acceleration, and y-acceleration at every instant in time $t_k = k*dt$, where dt = 20ms for our experiments. The Kalman model assumes that the cursor's states propagate in time according to the model

$$x_{k+1} = A_k x_k + w_k, \quad (1)$$

where k = 1,2,..., $A_k \in R^{6x6}$ is the coefficient matrix that linearly relates cursor kinematics (position, velocity, and acceleration) at time *k* to the next state at time *k* + 1. The body motion observations are assumed to be linearly related to the state via the stochastic linear function

$$z_k = H_k x_k + q_k, \quad (2)$$

where $z_k \in R^{24}$ is the 24 x 1 vector containing the motion sensor observations at each time step *k*. $H_k \in R^{Cx6}$ is the matrix that linearly relates the cursor's state to the body motion. The random variable w_k represents the process noise term which we assume has zero mean as is normally distributed, i.e. $w_k \sim N(0,W_k)$, $W_k \in R^{6x6}$. Additionally, q_k is the noise term in the observations, i.e. $q_k \sim N(0,Q_k)$, $Q_k \in R^{24x24}$.

In practice, A_k, H_k, W_k, and Q_k might change with time step *k*. However, we will make the common simplifying assumptions that they are normally distributed and remain constant. Therefore, we can estimate them from training data using maximum likelihood (for details, see [7]). Different variables in the estimated parameters are mapped to different units (position, velocity, acceleration), so analysis for overfitting and redundancy of our parameters is a subject that needs to be dealt with carefully in a separate study. One way to limit the risk of overfitting is by utilizing sufficiently long sequence of kinematic data in the calibration procedure. A discussion of the order of the kinematic variables and overfitting in the use of Kalman decoding for brain-machine interfaces can be found in [14].

C. Protocol

Eighteen healthy subjects (8 men, 10 female, 18-43 years) each gave their informed, signed consent to participate in this experiment, which was approved by Northwestern University's Institutional Review Board. Subjects were divided into three groups (six subjects each), a group with only Euler angles in the observation vector (E), a group with Euler angles and angular velocities (EV), and a group with angles, angular velocities, and linear accelerations (EVA).

1) Calibration—Subjects sat in front of a computer monitor while wearing the motion vest (Fig. 1). They were instructed to follow a moving cursor on an 18x18cm screen as if they were controlling it with their shoulders. The cursor made center-out movements to the east, north, west, and south directions, so they were instructed to "control" north and south by moving their right shoulder up and down (elevation and depression) respectively, and to "control" east and west by moving their left shoulder up and down respectively.

Each center-out movement had a cosine velocity profile so that the cursor's position history while moving east followed the function:

$$X_t = 5^* \sin(\pi/4^* t) \quad (3)$$

$$Y_t = 0 \quad (4)$$

where t = 0:0.02:4 so that the cursor moved from the origin to the east and then back to the origin. The cursor had a diameter of 1 cm and the movement range was enclosed by a 6x6cm box so that the subjects knew when the cursor would stop and start returning to the origin and they could plan to move their shoulder accordingly. Each of the four directions was reached a total of 6 times for a total training time of 96 seconds. Position, velocity, and acceleration of the cursor were recorded every 20ms along with the motion trackers' Euler angles, angular velocity, and linear accelerations. These data were taken as the Kalman filter's state and observation vectors respectively and they were used to estimate the model's parameters so that the cursor kinematics and body motion were now encoded by equations (1) and (2) respectively.

2) Practice—After subjects were assigned to a group and the parameters were estimated based on their group, they were now able to control a cursor on a screen by using only their body motions. Every subject had one minute to try their mapping by controlling a cursor on the screen. There was no specific task or goal, but they were suggested to try moving north and south repeatedly, then east and west, and finally make sure that they could reach all corners and edges of the screen.

Subjects had to move through their entire range of motion during the filter training phase. However, performing these types of movements during the whole length of the experiment might become strenuous, so we amplified their movements by 300% for the rest of the experiment. This means that subjects would have to move 33% of their shoulder motion range in order to reach a target located 5cm from the origin.

In order to improve stability and introduce a bias towards the origin like in a real joystick, the cursor was modeled as a joystick where the x and y outputs of the Kalman filter were modeled as forces acting on a mass spring damper system represented by the equation of motion:

$$s''+c/m^*s'+k/m^*s=0 \quad (5)$$

where $s = [x', y']^T_k$ represents the cursor's filtered new position coordinates. Values for the mass, spring, and damper coefficients were tuned so that the system had a resulting damping ration of

$$\zeta=c/2^*sqrt(m^*k)=0.1 \quad (6)$$

3) Reaching Task—Subjects performed center-out reaching movements to four different targets that appeared in random order on a 36×27 screen. Once the subject remained for 200ms on the origin, a 4 cm diameter yellow target appeared on the screen. The subjects were instructed to reach as quickly and accurately as possible and hold the cursor within the target for 1 second. The target turned green while the cursor was inside it and it turned red at a 5-second "deadline", where the trial was logged as a failed attempt and the target returned to the origin. Again, the subject had to move 33% of their shoulder motion range in order to reach the target 5cm from the origin.

Subjects performed 24 movements per epoch with random target order comprised of exactly six reaches in each direction. The experiment consisted on 5 epochs and there was a 30-60 resting period between them. This protocol allows us to chart an explicit learning curve of different performance measures with constant visual feedback.

D. Analysis/Statistics

a) *Error rate:* was defined the average number of failed attempts per trial.

b) *Movement time:* was computed as the total time it took for the subject to successfully complete the reaching task.

c) *Movement error:* was the average distance from the sample points to the task axis, irrespective of whether the points were above or below the axis.

d) *Maximum error:* was calculated as the maximum absolute deviation of the points from the task axis.

e) *Movement variability:* measured the extent to which the sample points lie in a straight line along an axis parallel to the task axis and was calculated by the standard deviation.

f) *Path length:* was computed as the sum of the Euclidian distance between time-consecutive points along the reach.

All performance measures were averaged over all movements by epoch. This produced a total of five values per performance measure for each subject for the whole experiment. Together, these performance measures allow us to elicit differences in the cursor's path and

control between the three different groups. The standard error between subjects in each group was calculated for the error bars shown in Fig. 3.

A two-factor, mixed-model analysis of variance (ANOVA) for repeated measures with each performance measure as the dependent repeated measure, and group and epoch as the two independent factors, was used to test the null-hypothesis that the mean between groups at each epoch was the same. This test was repeated for each performance measure and allows us to reject the null-hypothesis at each epoch at $p<0.05$.

A two-way mixed model analysis of variance (ANOVA) was performed on each performance measure with EPOCH (1, 2, 3, 4, 5) as the within-participant factor and GROUP (E EV, and EVA) as the between-participant factor. Corrected violations of sphericity were performed using the Greenhouse-Geisser correction. Post-hoc comparisons using a Bonferroni correction were performed to test the null-hypotheses that the mean *between* groups at each epoch was the same, and that the mean for the first and last epochs *within* the same group was the same. These tests were repeated for each performance measure and allowed us to reject the null-hypothesis at each epoch at $p<0.05$.

III. RESULTS

As subjects practiced controlling a cursor on the screen by shoulder motions, their movements became more accurate. Fig. 2 illustrates a general increase in task performance and movement linearity in sample trajectories from a typical subject in each group. The left and right panels show reaching trajectories at the first and last epochs of the experiment. Reaches to each direction are represented by a different color. Prior to training, controlling the cursor was extremely difficult for subjects in groups E, and EV, as shown by erratic looking trajectories and high errors in panels a and c of Fig 2. Control before training was not as complicated for subjects in group EVA, as illustrated in panel e. After training, subjects in all groups exhibit well-established and quasi-linear movements of the cursor. This is consistent with evidence suggesting that linear trajectories will dominate the control strategy of subjects in reaching movements where visual feedback is available [15–18].

a) *The data indicate that final error rate* after five epochs was reduced to approximately 70% ($p = 1.00$), of the initial error rate for subjects in the E group and 24% ($p = 0.04$) and 83% ($p = 1.00$) for groups EV and EVA respectively. These final levels or performance correspond to 0.229+/−0.004 failed trials/trials, 0.073+/−0.003 failed trials/trials, and 0.059+/−0.002 failed trials/trials for subjects in groups E, EV, and EVA respectively (values are means +/− 95% confidence). The E and EV groups reduced error rate faster than the EVA group but groups EV and EVA ultimately seemed to converge to the same level of final performance (Fig 3-a).

b) *The movement time* that subjects took to complete the each reaching movement was also demonstrated, and the subjects in groups E, EV, and EVA reduced their movement times to 86% ($p = 0.67$), 71% ($p = 0.01$), and 91% ($p = 1.00$) of their initial times by the fifth epoch respectively. This corresponds to average final

movement times of 3.31+/−0.02 sec, 2.63+/−0.01 sec, and 2.34+/−0.02 sec for groups E, EV, and EVA respectively (Fig 3-b).

c) *Movement error* was reduced to 73% (p = 0.14), 64% (p = 0.03), and 98% (p = 1.00) of the initial performance of subjects in groups E, EV, and EVA respectively. The average final movement error for subjects in groups E, EV, and EVA was of 0.94+/−0.007 cm, 0.80+/−0.005 cm and 0.66+/−005 cm (Fig 3-c).

d) *Maximum error* on the fifth epoch was 71% (p = 0.15) of the error on the initial epoch for group E and 65% (p = 0.07) and 97% (p = 1.00) for groups EV and EVA respectively. The final maximum error corresponds to 2.31+/−0.02 cm, 1.93+/−0.02 cm, and 1.47+/−0.01 cm for subjects in groups E, EV, and EVA respectively, (Fig 3-d).

e) *Movement variability* of subject's reaches decreased as they became more familiar with the control of the cursor using their shoulders. After the five epochs, subjects in groups E, EV, and PA reduced their variability to approximately 73% (p = 0.10), 70% (p = 0.11) and 96% (p = 1.00) of their variability in the first epoch. These values correspond to a variability of 0.90+/−0.006 cm, 0.76+/−0.006 cm, and 0.55+-/0.005 cm for groups E, EV, and EVA respectively (Fig 3-e).

f) *Path length* showed a similar improvement in performance with subjects in groups E, EV, and EVA reducing their path lengths to 74% (p = 0.16), 67% (p = 0.08) and 93% (p = 1.00) of their initial performances by the fifth epoch. These path lengths correspond to 13.84+/−0.14 cm, 11.08+/−0.04 cm, and 9.34+/−0.08cm for subjects in groups E, EV, and EVA respectively, (Fig 3-f).

Between-groups comparison at each epoch failed to show statistical significance for the most part (Table 1). Significant differences were only apparent in some epochs between groups E and EVA (p-values in bold on the table), which are the groups with the least and the most information in the observation vector respectively.

IV. CONCLUSION

We investigated whether a discrete linear Kalman filter algorithm based on upper-body motion could help subjects learn to operate a virtual cursor. Our goal was extending to body-machine interfaces an approach to decoding that has been first proposed for brain-machine interfaces [7]. In our experiment, Euler angles, angular velocities, and linear accelerations of the shoulders served as the algorithm's observation and were linearly mapped to the virtual cursor's kinematics, or the model's state. This approach has a well-understood theory [5] and its rigorous probabilistic method of on-line recursive estimation provides a computationally efficient filter algorithm.

Subjects in the EVA group achieved a better performance with less training than subjects in the other two groups. However, subjects in the EV group ultimately reached the same level of performance as subjects in EVA after extended training. Interestingly, subjects in the

EVA group failed to improve their performance after prolonged training. This might indicate that subjects in this group reached a ceiling in performance early in the experiment. Increasing the level of challenge during the reaching task i.e. reaching in directions that require combinations of movements, might elicit a more explicit improvement in proficiency for this group.

This study investigated the importance of exploiting the abundance and redundancy of body motions for the effective control of a cursor's kinematics. In order to remove variability caused by individual's control choices, we standardized the “control” strategy that subjects used so that they all moved the cursor north and south with their right shoulder and east and west with their left shoulder. Every type of injury to the cervical spinal cord is distinct, and subjects with high tetraplegia will have unique residual motion and upper-body coordination, therefore we can't expect all of them to have equal abilities and preferences in performing upper-body motions. Future experiments will let subjects make their own choices of control strategies to move the cursor north, south, east, and west.

Different methods have been proposed for people with high tetraplegia to control their powered wheelchairs. Inertial Measurement Units were mounted at the back of a user's head while orientation values were converted into adequate, steering commands [19]. This method provides an intuitive, easy to implement, and computationally efficient control of a wheelchair. However, interaction with the interface is constrained to the head only and therefore fails to promote upper-body coordination, when the users may still have significant residual motion capability. Electroencephalography (EEG) methods for the control of a powered wheelchair have also been investigated by different groups [20], [21]. However, these methods are more computationally expensive and require a high concentration and long familiarization phase from the user. Additionally, users have to rely on external cues and the wheelchair follows a predetermined path [20].

Our goal is to develop a non-invasive body machine interface that will adapt to each user's unique residual shoulder motion. To develop this interface, we performed preliminary experiments on unimpaired subjects. One should not assume that these findings can be extrapolated to people with paralysis. We have begun to test the system on spinal cord injured participants and we plan to publish the findings as they will become available. The future direction of our work is to develop customized interfaces so that subjects can use their mapped virtual cursor to communicate with a keyboard, a joystick and a keypad. This will allow subjects to practice and improve their control while browsing the internet, writing e-mails, playing video games, performing increasingly challenging reaching tasks, and practice the control of a wheelchair inside a safe and controlled virtual reality environment. Enough training and continued use of upper-body coordination might help people who suffered an injury to the cervical spinal cord to avoid or minimize comorbidities of paralysis and recover some of the lost mobility.

Acknowledgments

This work was supported by: NSF Grant DGE-0824162, NICHHD Grant 1R01HD072080, NIDRR Grant H133E120010, the Ralph and Marian C Falk Medical Research Trust, the Craig H Neilsen Foundation, and the Brinson Foundation.

References

1. Hesse S, Schmidt H, Werner C, Bardeleben A. Upper and lower extremity robotic devices for rehabilitation and for studying motor control. Current opinion in neurology. Dec.2003 16(6):705–10. [PubMed: 14624080]
2. Chen R, Corwell B, Yaseen Z, Hallett M, Cohen LG. Mechanisms of cortical reorganization in lower-limb amputees. The Journal of neuroscience : the official journal of the Society for Neuroscience. May; 1998 18(9):3443–50. [PubMed: 9547251]
3. Chen R, Cohen LG, Hallett M. Nervous system reorganization following injury. Neuroscience. Jan. 2002 111(4):761–73. [PubMed: 12031403]
4. Paninski L, Fellows MR, Hatsopoulos NG, Donoghue JP. Spatiotemporal tuning of motor cortical neurons for hand position and velocity. Journal of neurophysiology. Jan.2004 91(1):515–32. [PubMed: 13679402]
5. Welch G, Bishop G. An Introduction to the Kalman Filter. 2006:1–16.
6. Brown EN, Frank LM, Tang D, Quirk MC, Wilson MA. A Statistical Paradigm for Neural Spike Train Decoding Applied to. 1998; 18(18):7411–7425.
7. Wu W, Black M, Gao Y. Inferring hand motion from multi-cell recordings in motor cortex using a Kalman filter. SAB'02Workshop on Motor Control in Humans and Robots: On the Interplay of Real Brains and Artificial Devices. 2002
8. Fehr L, Langbein WE, Skaar SB. Adequacy of power wheelchair control interfaces for persons with severe disabilities: a clinical survey. Journal of rehabilitation research and development. 2000; 37(3):353–60. [PubMed: 10917267]
9. Wolpaw JR, McFarland DJ. Control of a two-dimensional movement signal by a noninvasive brain-computer interface in humans. Proceedings of the National Academy of Sciences of the United States of America. Dec.2004 101(51):17849–54. [PubMed: 15585584]
10. Lotte F, Congedo M, Lécuyer a, Lamarche F, Arnaldi B. A review of classification algorithms for EEG-based brain-computer interfaces. Journal of neural engineering. Jun.2007 4(2):R1–R13. [PubMed: 17409472]
11. Chestek, C. a; Cunningham, JP.; Gilja, V.; Nuyujukian, P.; Ryu, SI.; Shenoy, KV. Neural prosthetic systems: current problems and future directions.. Conference proceedings : ... Annual International Conference of the IEEE Engineering in Medicine and Biology Society. IEEE Engineering in Medicine and Biology Society. Conference; Jan.. 2009 p. 3369-75.
12. Kim S-P, Simeral JD, Hochberg LR, Donoghue JP, Friehs GM, Black MJ. Point-and-click cursor control with an intracortical neural interface system by humans with tetraplegia. IEEE transactions on neural systems and rehabilitation engineering : a publication of the IEEE Engineering in Medicine and Biology Society. Apr.2011 19(2):193–203.
13. Orsborn AL, Dangi S, Moorman HG, Carmena JM. Closed-loop decoder adaptation on intermediate time-scales facilitates rapid BMI performance improvements independent of decoder initialization conditions. IEEE transactions on neural systems and rehabilitation engineering : a publication of the IEEE Engineering in Medicine and Biology Society. Jul.2012 20(4):468–77.
14. Wu W, Gao Y, Bienenstock E, Donoghue JP, Black MJ. Bayesian population decoding of motor cortical activity using a Kalman filter. Neural computation. Jan.2006 18(1):80–118. [PubMed: 16354382]
15. Danziger Z, Fishbach A, Mussa-Ivaldi F. a. Learning algorithms for human-machine interfaces. IEEE transactions on bio-medical engineering. May; 2009 56(5):1502–11. [PubMed: 19203886]
16. Hogan N. An organizing principle for a class of voluntary movements. The Journal of Neuroscience. 1984; 4(11):2745–2754. [PubMed: 6502203]
17. Wolpert DM, Ghahramani Z, Jordan MI. Are arm trajectories planned in kinematic or dynamic coordinates? An adaptation study. Experimental brain research. Experimentelle Hirnforschung. Expérimentation cérébrale. Jan.1995 103(3):460–70.
18. Flanagan J, Rao A. Trajectory adaptation to a nonlinear visuomotor transformation: evidence of motion planning in visually perceived space. Journal of neurophysiology. 1995
19. Mandel C, Rofer T, Frese U. Applying a 3dof orientation tracker as a human-robot interface for autonomous wheelchairs. Rehabilitation Robotics. 2007; 00(c):52–59. 2007.

20. Iturrate I, Antelis J. A noninvasive brain-actuated wheelchair based on a P300 neurophysiological protocol and automated navigation. IEEE Transactions on Robotics. 2009; 25(3):614–627.

21. Carlson T, Millán JDR. The Robotic Architecture of an Asynchronous Brain–Actuated Wheelchair. IEEE Robotics and Automation Magazine. 2012; 20(1):65–73.

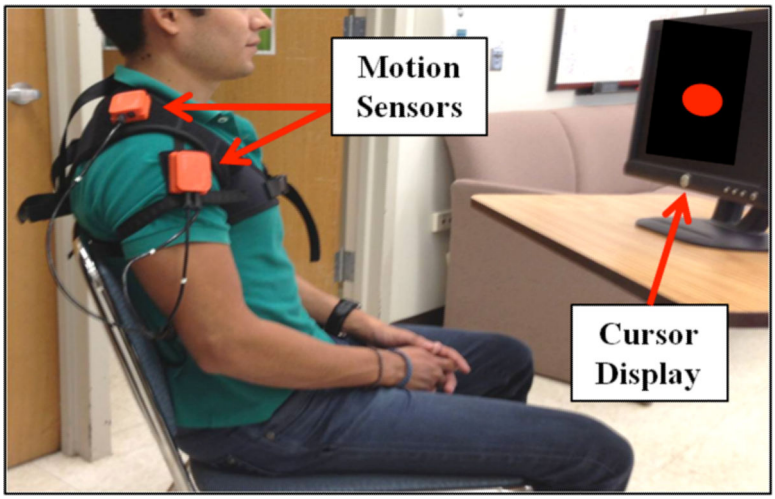

Fig. 1. Experimental setu for learning

The subject sits in front of a visual display wearing the four Inertial Measurement Units. A virtual cursor moves with known kinematics and the subject is instructed to move as if he was controlling it with his shoulders.

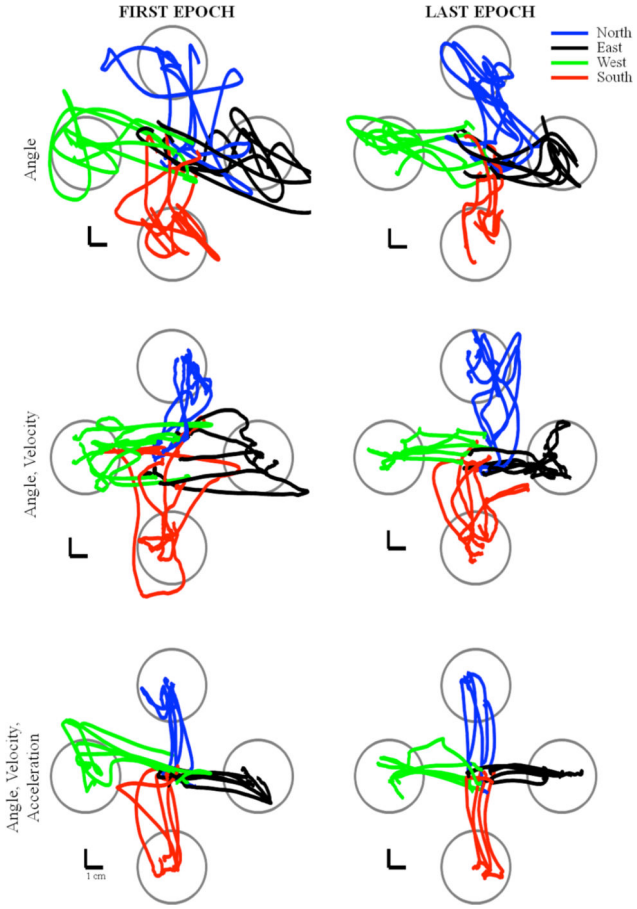

Fig. 2. Reaching paths for the first and last epochs for representative subjects in each group

Each reaching direction is depicted in a different color. The task was very challenging during the first epoch for subjects in groups E and EV, but not so much for subjects on group EVA. Reaching error and variability reduced after training for all groups.

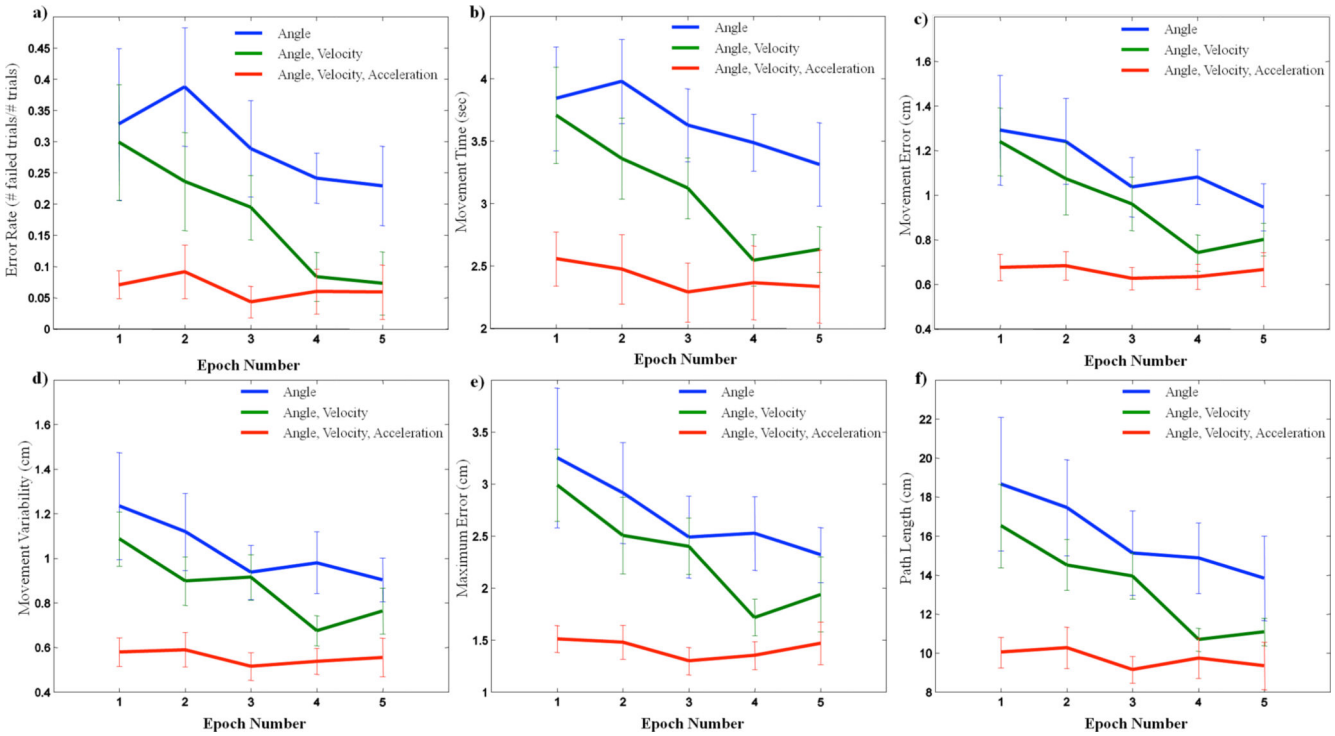

Fig. 3. Performance averages for each epoch with each group represented on a different color

Subjects in all groups improved their performance after five epochs of training. Groups E and EV (blue and green respectively) improved faster and more dramatically than group EVA. The error bars represent the standard error for each group

Table 1

The p-value for the between-groups comparison at each epoch is shown in each performance measure's table. The error rate p-value for the comparison between groups E and EVA during the third epoch was 0.04.

Error Rate																Movement Time														Movement Error													
Epoch	**1**			**2**			**3**			**4**			**5**			**Epoch**	**1**			**2**			**3**			**4**			**5**			**Epoch**	**1**			**2**			**3**			**4**			**5**		
Group	**A**	**AV**	**AVA**	**A**	**AV**	**AVA**	**A**	**AV**	**AVA**	**A**	**AV**	**AVA**	**A**	**AV**	**AVA**	**Group**	**A**	**AV**	**AVA**	**A**	**AV**	**AVA**	**A**	**AV**	**AVA**	**A**	**AV**	**AVA**	**A**	**AV**	**AVA**	**Group**	**A**	**AV**	**AVA**	**A**	**AV**	**AVA**	**A**	**AV**	**AVA**	**A**	**AV**	**AVA**	**A**	**AV**	**AVA**
A	-	1.00	0.25	-	0.64	0.07	-	0.87	**0.04**	-	0.05	**0.02**	-	0.23	0.17	A	-	1.00	0.09	-	0.67	**0.02**	-	0.69	**0.01**	-	0.08	**0.03**	-	0.40	0.11	A	-	1.00	0.10	-	1.00	0.09	-	1.00	0.08	-	0.09	**0.02**	-	0.90	0.16
AV	-	-	0.36	-	-	0.71	-	-	0.30	-	-	1.00	-	-	1.00	AV	-	-	0.16	-	-	0.26	-	-	0.16	-	-	1.00	-	-	1.00	AV	-	-	0.15	-	-	0.34	-	-	0.18	-	-	1.00	-	-	0.98

Movement Variability																Maximum Error														Path Length													
Epoch	**1**			**2**			**3**			**4**			**5**			**Epoch**	**1**			**2**			**3**			**4**			**5**			**Epoch**	**1**			**2**			**3**			**4**			**5**		
Group	**A**	**AV**	**AVA**	**A**	**AV**	**AVA**	**A**	**AV**	**AVA**	**A**	**AV**	**AVA**	**A**	**AV**	**AVA**	**Group**	**A**	**AV**	**AVA**	**A**	**AV**	**AVA**	**A**	**AV**	**AVA**	**A**	**AV**	**AVA**	**A**	**AV**	**AVA**	**Group**	**A**	**AV**	**AVA**	**A**	**AV**	**AVA**	**A**	**AV**	**AVA**	**A**	**AV**	**AVA**	**A**	**AV**	**AVA**
A	-	1.00	0.05	-	0.83	**0.05**	-	1.00	**0.04**	-	0.17	**0.03**	-	1.00	0.10	A	-	1.00	0.07	-	1.00	0.07	-	1.00	**0.05**	-	0.14	**0.02**	-	1.00	0.22	A	-	1.00	0.10	-	0.86	**0.05**	-	1.00	0.06	-	0.14	0.53	-	0.75	0.21
AV	-	-	0.17	-	-	0.41	-	-	0.06	-	-	1.00	-	-	0.55	AV	-	-	0.14	-	-	0.27	-	-	0.08	-	-	1.00	-	-	0.91	AV	-	-	0.30	-	-	0.39	-	-	0.16	-	-	1.00	-	-	1.00